

Received:
12 May 2017Revised:
06 September 2017Accepted:
11 September 2017<https://doi.org/10.1259/bjr.20170350>

Cite this article as:

Park S, Kwack K-S, Lee YJ, Gho S-M, Lee HY. Initial experience with synthetic MRI of the knee at 3T: comparison with conventional T_1 weighted imaging and T_2 mapping. *Br J Radiol* 2017; **90**: 20170350.

FULL PAPER

Initial experience with synthetic MRI of the knee at 3T: comparison with conventional T_1 weighted imaging and T_2 mapping

^{1,2}SUNGHOO PARK, MD, ^{1,2}KYU-SUNG KWACK, MD, ³YOUNG JU LEE, Ph.D., ³SUNG-MIN GHO, Ph.D. and ^{4,5}HYUN YOUNG LEE, Ph.D.

¹Department of Radiology, Ajou University School of Medicine, Suwon, South Korea

²Musculoskeletal Imaging Laboratory, Ajou University Medical Centre, Suwon, South Korea

³Department of Clinical Science, GE Healthcare, Seoul, South Korea

⁴Regional Clinical Trial Centre, Ajou University Medical Centre, Suwon, South Korea

⁵Department of Biostatistics, Yonsei University College of Medicine, Seoul, South Korea

Address correspondence to: Kyu-Sung Kwack

E-mail: xenoguma@gmail.com; xenoguma@ajou.ac.kr

Objective: To assess the feasibility and accuracy of synthetic MRI compared to conventional T_1 weighted and multi-echo spin-echo (MESE) sequences for obtaining T_2 values in the knee joint at 3 Tesla.

Methods: This retrospective study included 19 patients with normal findings in the knee joint who underwent both synthetic MRI and MESE pulse sequences for T_2 quantification. T_2 values of the two sequences at the articular cartilage, bone marrow and muscle were measured. Relative signal intensity (SI) of each structure and relative contrast among structures of the knee were measured quantitatively by T_1 weighted sequences.

Results: The mean T_2 values for cartilage and muscle were not significantly different between MESE pulse sequences and synthetic MRI. For the bone marrow, the mean T_2 value obtained by MESE sequences (124.3 ± 3.6 ms) was significantly higher than that obtained

by synthetic acquisition (73.1 ± 5.3 ms). There were no significant differences in the relative SI of each structure between the methods. The relative contrast of bone marrow to muscle was significantly higher with conventional T_1 weighted images, while that for bone marrow to cartilage was similar for both sequences.

Conclusion: Synthetic MRI is able to simultaneously acquire conventional images and quantitative maps, and has the potential to reduce the overall examination time. It provides comparable image quality to conventional MRI for the knee joint, with the exception of the bone marrow. With further optimization, it will be possible to take advantage of the image quality of musculoskeletal tissue with synthetic imaging.

Advances in knowledge: Synthetic MRI produces images of good contrast and is also a time-saving technique. Thus, it may be useful for assessing osteoarthritis in the knee joint in the early stages.

INTRODUCTION

MRI provides high soft tissue contrast and can be used to assess the internal derangement of joints. However, MRI scans can take a long time, and unlike CT, the signal intensities (SIs) obtained with conventional MRI are not quantitative. Therefore, the intensities of pathological processes obtained by this technique can neither be used as a comparison for follow-up examinations nor can they be compared to reference normal values.¹

SyMRI is a synthetic MRI method based on a quantitative approach in which a single saturation recovery turbo spin echo sequence is used to estimate absolute physical properties, proton density (PD), longitudinal relaxation

rate and transverse relaxation rate, including correction for B1 inhomogeneities.² Rather than predetermining the acquisition parameters such as echo time (TE), repetition time (TR) and inversion time, to maximize tissue contrast, synthetic MRI produces a free range of synthetic weightings based on a single sequence through mathematical inference.³⁻⁵ The quantitative sequences used in synthetic MRI measure inherent tissue properties (T_1 , T_2 and PD), and these measurements can be used for individual patient follow-up and comparison between patients.

The clinical use of synthetic MRI has been demonstrated in the brain in various disease processes.^{1,2,6-8} However, there have been no reports regarding its application to the

musculoskeletal system. In this study, we assessed the image contrast of synthetic MRI compared to corresponding conventionally obtained clinical MRIs of the knee joint. This study was performed to assess the T_2 values in the knee, as measured by synthetic MR sequences compared to 2D fast spin-echo (FSE) multi-echo spin-echo (MESE) sequences. The secondary aim was to evaluate synthetic MRI in a clinical setting by assessing the relative SI and contrast compared to conventional T_1 weighted images.

METHODS AND MATERIALS

Case selection

This study received Institutional Review Board approval, and the requirement for informed consent was waived. The study population consisted of 218 consecutive patients who had undergone knee MRI from March 2016 to May 2016. The inclusion criteria were normal knee MRI findings in the routine protocol sequences with additional synthetic sequences, comparable conventional T_1 weighted sequences and 2D FSE MESE sequences used for T_2 mapping. Patients with the following abnormal findings were excluded: osteoarthritis with or without meniscal degeneration or tear ($n = 103$), substantial trauma with fracture or ligament injury ($n = 44$), inappropriate MR protocol ($n = 23$), previous operative status ($n = 11$), septic or inflammatory arthritis ($n = 10$) and bone or soft tissue tumour ($n = 8$). Thus, a total of 19 patients were included and evaluated in this retrospective study. The mean age was 39.3 years (range, 17–54 years); 12 patients were males and 7 were females.

MR parameters

All of the MR studies were acquired on a 3.0 T MR unit (Discovery MR750W; GE Healthcare, Waukesha, WI) using a transmit-receive quadrature knee coil (GE Healthcare). Sagittal T_1 weighted, 2D FSE MESE sequences for T_2 mapping and

synthetic MR sequences were acquired during clinical MRI in addition to the conventional MRI sequences in the knee at our institution. The imaging parameters of each sequence are summarized in Table 1.

Synthetic MRI was performed using MAGiC, which is a customized version of SyntheticMR's SyMRI software. The MAGiC sequences are 2D FSE multi dynamic, multi-echo sequences that use an interleaved slice-selective 120° saturation and multi-echo acquisition, and images are obtained with different combinations of TE and saturation delay time. Each acquisition led to eight complex images per section with different combinations of four saturation delays and two TEs. The acquisition time of the synthetic MR sequences was 5 min, 36 s. Sagittal conventional T_1 weighted and MESE sequences for T_2 values were acquired with section thickness and in-plane resolution matching those of the synthetic MR sequences. Imaging parameters (TR, TE) were also selected to provide visual image contrast similar to the synthetic MR images. T_2 quantification sequences were obtained using a sagittal MESE acquisition with eight TEs (7.2, 14.4, 21.6, 28.8, 36, 43.2, 50.4 and 57.6 ms). The T_2 map from MESE was obtained using dedicated software (Discovery 750w, T_2 Map; GE Healthcare). Synthetic T_1 weighted images and T_2 maps were created from raw quantification data with SyMRI software in the GE 3T scanner console. Figure 1 shows examples of a conventional T_1 weighted image, a T_2 map and synthetic MR images.

Image analysis

Quantitative assessment was performed using a picture archiving and communication system and Advantage Workstation (GE Healthcare). In all of the subjects, the regions of interest (ROIs) were measured for cartilage, bone and muscle.^{9,10} ROIs on a sagittal plane were positioned on the superior lateral trochlear

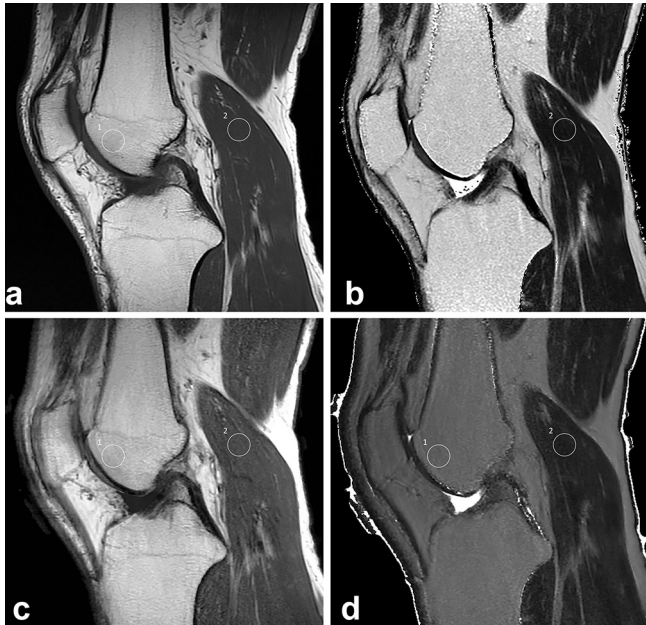
Table 1. MR parameters

Imaging parameter	Synthetic	Conventional T_1	MESE
Acquisition plane	Sagittal	Sagittal	Sagittal
Field of view (cm)	16	16	16
Matrix	320 × 224	320 × 224	320 × 224
Section thickness (mm)	4.0	4.0	4.0
Slices	24	24	24
Interslice gap (mm)	0.4	0.4	0.4
Flip angle	120	90	90
TR (ms)	4000 ^a	640–800	800
TE (ms)	22, 90 ^a	7	7.2, 14.4, 21.6, 28.8, 36, 43.2, 50.4, 57.6
Echo train length	12	3	1
Bandwidth (Hz/pixel)	81.37	162.77	244.14
Number of excitations	1	2	1
Parallel factor	2	1	1
Acquisition time	5 min 36 s	1 min 40 s	9 min 3 s

MESE, multi-echo spin-echo; TE, echo time; TR, repetition time.

^aAcquisition parameters. Synthetic images were generated using TR and TE matching the conventional or traditional sequences.

Figure 1. Example of conventional and synthetic images of the knee. (a) Conventional T_1 weighted image (TR/TE = 650/7). (b) T_2 map from the MESE sequences (scale 25–75 ms). Standard conventional images are shown in the top row (a, b), and the corresponding synthetic images for the same patients are shown in the bottom row (c, d). Regions of interest were placed within the superior lateral trochlear cartilage (not shown), medial femoral condyle in the first full slice from the intercondylar notch for bone (1) and gastrocnemius muscle medial head (2). MESE, multi-echo spin-echo; TE, echo time; TR, repetition time.

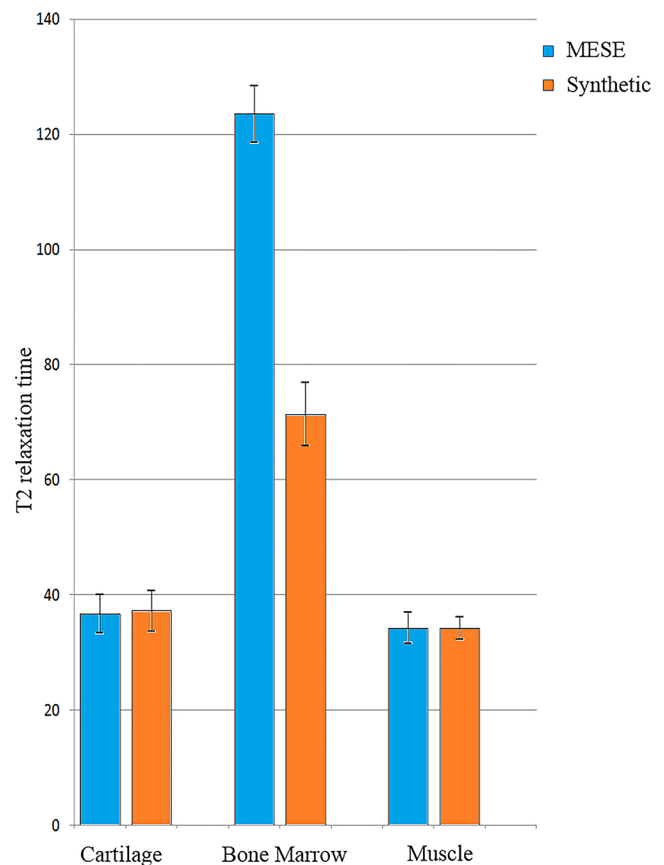


cartilage, medial femoral condyle in the first full slice from the intercondylar notch for bone and gastrocnemius muscle medial head, as done in previous studies.^{9,11} The circular ROI for cartilage measurement was 3 mm in diameter, and that for the bone marrow and muscle was 9 mm in diameter.¹² ROIs for each patient were identical in size and placed in identical positions on matching sections. Each measurement was performed by two radiologists with 14 and 9 years of experience, respectively. To secure reproducibility, tiny dots were marked and recorded at the point of the previously measured area by the first reader. The second reader measured the values with ROIs around the dots.¹³ We measured the mean T_2 values at each ROI on the T_2 map generated from both MESE and synthetic MR sequences, and compared the differences in T_2 values between the two sequences. The means and standard deviation of the SI within each ROI on conventional and synthetic T_1 weighted MR images were recorded. The relative SI and relative contrast were used for direct comparison of image quality between the conventional and synthetic T_1 weighted images. The relative SI of each structure was calculated as SI/SD , and the relative contrast of structure A (a) to structure B (b) was calculated as $(SI_a - SI_b) / (SD_a^2 + SD_b^2)^{1/2}$ ^{14–16}

Statistical analysis

To assess differences between measurements of T_2 values, we generated Bland–Altman plots for plotting the difference

Figure 2. Means and standard deviations of T_2 values for multi-echo spin-echo and synthetic MR sequences.

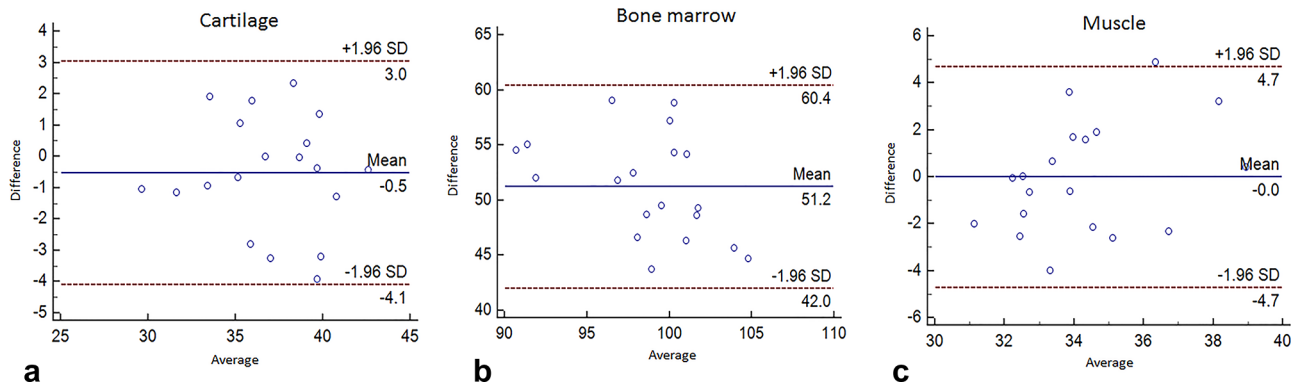


between measurements (y-axis) and mean of measurements (x-axis). The horizontal dashed lines reflect the mean difference between measurements ($2 \times SD$ of difference in measurements). The interobserver agreement of T_2 values between MESE and synthetic MR sequences was quantified using the intraclass correlation coefficient. The r values were classified as follows: 1.0, perfect agreement; 0.81–0.99, almost perfect agreement; 0.61–0.80, substantial agreement; 0.41–0.60, moderate agreement; 0.21–0.40, fair agreement; and ≤ 0.20 , slight agreement.¹⁷ Wilcoxon's signed-rank test was used to determine if there were statistically significant differences in relative SI and relative contrast obtained with conventional and synthetic T_1 weighted images. Statistical analyses were performed using the SPSS (ver. 22; IBM corp., Armonk, NY) and MedCalc (ver. 16; MedCalc, Ostend, Belgium) software packages. In all of the analyses, $p < 0.05$ was taken to indicate statistical significance.

RESULTS

For cartilage and muscle, the mean T_2 values in the MESE sequences were slightly lower than those in the synthetic MR sequences. However, the differences were not statistically significant (cartilage, 36.7 ± 3.4 ms and 37.2 ± 3.5 ms, $p = 0.686$; muscle, 34.2 ± 2.7 ms and 34.3 ± 2.0 ms, $p = 0.863$). The mean T_2 value of bone marrow was significantly higher for MESE (124.3 ± 3.6 ms, $p < 0.001$) than for synthetic MR sequences (73.1 ± 5.3 ms) (Figure 2). Bland–Altman plots indicated good agreement between the sequences, as demonstrated by the small differences

Figure 3. Bland-Altman plots of T_2 values of cartilage (a) bone marrow (b) and muscle (c). The y- and x-axes indicate the difference and average between multi-echo spin-echo and synthetic MR sequences, respectively. The blue lines show the means of differences, while the 95% confidence intervals are denoted by the pairs of dotted red lines.



between T_2 values of cartilage and muscle. The mean differences in T_2 values were -0.5 ± 3.5 ms at the cartilage and 0 ± 4.7 at the muscle (Figure 3). The interobserver agreements for each parameter are summarized in Table 2. The T_2 values for cartilage, bone marrow and muscle exhibited substantial or almost perfect agreement.

The mean values for the relative SI of each structure and relative contrast of bone marrow to cartilage and bone marrow to muscle are shown in Table 3. There were no significant differences among the structures, although the mean relative SI for cartilage and muscle were slightly higher for the conventional T_1 weighted sequences, except in the bone marrow. The relative contrast of bone marrow to cartilage in the synthetic sequences was similar to that for the conventional T_1 weighted sequences. The conventional T_1 weighted sequences showed significantly higher relative contrast of bone marrow to muscle compared to the synthetic MR sequences ($p = 0.011$).

DISCUSSION

The MAGiC sequence is very fast; the data are acquired in a single scan, the image contrast can be adjusted after scanning by manipulating TR, TE and inversion time, and quantitative maps provide absolute values of the physical properties of patients. The majority of the literature regarding synthetic MRI and its clinical application has focused on the pathology of the

brain. In our initial experience with this technique in the knee joint, we showed that synthetic MRI in the knee yields similar T_1 weighted contrast and T_2 values as conventionally acquired images, suggesting that it may be useful for evaluating the internal derangement of the knee joint.

MRI acquisition time is critical in the musculoskeletal area. Compared to other anatomical structures, the PD-weighted sequences, which has excellent signal distinction among fluid, hyaline cartilage and fibrocartilage are essential for the assessment of joints. Furthermore, an additional imaging plane that has an oblique orientation for evaluating structures such as ligaments may add time to the examination and limit workflow. Several authors^{18–22} have reported that a 3D sequence capable of reformatting in various planes is a promising method for imaging the musculoskeletal system and would allow faster isotropic acquisition of musculoskeletal MR images. Previous studies^{23,24} have shown that the mDixon technique rapidly generates multiple images in a single acquisition, and the use of mDixon images as substitutes for T_2 weighted images and fat-suppressed T_2 weighted images would reduce the total examination time. In addition, Andreisek et al²⁵ reported that image generation with the synthetic TE technique was a potentially viable alternative to standard T_2 weighted images obtained at different TEs for evaluation of meniscus and articular cartilage in the knee joint. Where previous studies have focused mostly

Table 2. Intraclass correlation coefficient for agreement between MESE and synthetic MR sequences for T_2 values

		MESE	Synthetic
Cartilage	Spearman correlation (ρ)	0.740 (0.326–0.900)	0.731 (0.303–0.897)
	<i>p</i> -value	0.003	0.004
Bone marrow	Spearman correlation (ρ)	0.763 (0.386–0.909)	0.762 (0.393–0.908)
	<i>p</i> -value	< 0.001	0.002
Muscle	Spearman correlation (ρ)	0.814 (0.516–0.928)	0.655 (0.121–0.866)
	<i>p</i> -value	< 0.001	0.016

MESE, multi-echo spin-echo.

Numbers in parentheses are 95% confidence intervals.

Table 3. Comparison of the relative SI of each structure and relative contrast between conventional T_1 weighted and synthetic MR images

	Conventional T_1	Synthetic T_1	p -value
Relative SI			
Cartilage	17.2 ± 7.5	15.2 ± 6.1	0.370
Bone marrow	12.1 ± 3.8	13.8 ± 3.1	0.075
Muscle	13.3 ± 4.9	12.0 ± 3.8	0.418
Relative contrast			
Bone marrow to cartilage	7.3 ± 2.9	6.7 ± 2.0	0.624
Bone marrow to muscle	7.5 ± 2.0	6.1 ± 1.6	0.011

SI, signal intensity.

on reducing the time of sequences associated with T_2 contrast, synthetic MR sequences provide synthesized images including T_2 and PD-weighted sequences as well as T_1 weighted sequences, and also generate quantitative measurements such as T_1 and T_2 relaxation maps.

T_2 mapping sequences have been commonly used to assess the articular cartilage of the knee joint.^{26–28} The T_2 value for articular cartilage reflects the water content, collagen content and collagen fibre orientation in the extracellular matrix, with longer T_2 values thought to represent cartilage degeneration.^{27,29–32} In this study, the accuracy and reproducibility of T_2 values using the synthetic sequences were evaluated in knee joints. We found that the T_2 values of cartilage and muscle in the knee joint, calculated from the synthetic MR sequences, were highly consistent with those calculated by the MESE sequences. Although the value of bone marrow was significantly different for the synthetic sequences, the accuracy and reproducibility of T_2 relaxation times of the knee joint, including cartilage, muscle and bone marrow were substantial or almost perfect. The differences in relative SI and contrast between conventional T_1 weighted and synthetic MR sequences showed similar results. In contrast to cartilage and muscle, relative SI of bone marrow and relative contrast of bone marrow to muscle were significantly different for the synthetic MR sequence. The significant differences in relative SI and relative contrast in the bone marrow may be mainly attributable to the lack of optimization for musculoskeletal tissues in the synthetic sequences, and/or the inherent limitations of the MAGiC sequences (e.g. the limited relaxation points). In a clinical setting, MAGiC sequences allow one to choose the field of view, matrix size, slice thickness, slice gap and acceleration factor. The echo train length can be chosen in a limited range of 10–16. The TR has a minimum value of 4000 ms. The TEs are chosen automatically (approximately 20 and 95 ms). Therefore,

the SI of the musculoskeletal tissue, such as bone marrow, subcutaneous fat and meniscus, which have very long or short T_2 values, can be measured as unexpected values for the inherent properties of musculoskeletal tissue. The results could also be due to differences in the acceleration factor for parallel imaging. Future technical efforts should be directed towards optimization for musculoskeletal application.

There were several limitations in this study. First, our study included a small number of patients with only normal findings in knee MRI. Additional studies are necessary to compare the diagnostic abilities of synthetic and conventional sequences for the detection of various pathological conditions of internal derangement of the knee. Second, we did not evaluate synthetic sequences from T_2 weighted and PD-weighted images. Third, in this study, ROI measurements in musculoskeletal tissues showing low signal intensities were not performed because the current MAGiC sequence has not been optimized for tissues with low T_2 values such as the meniscus or ligaments. Fourth, based on our results indicating differences in the SI of bone marrow and relative contrast of bone marrow to muscle in the synthetic MR sequences, there is a potential limitation in the assessment or comparison of subchondral bone marrow oedema associated with osteochondral lesions between initial and follow-up studies.

In summary, synthetic MRI is a promising new MRI technique that obtain multi-contrast images simultaneously, making it ideal for evaluating the knee joint. Although evaluation of musculoskeletal tissues with high T_2 values, such as bone marrow, is limited, this method would be very useful for quantitatively studying and diagnosing diseases of the musculoskeletal system after further optimization. To the best of our knowledge, this is the first application of synthetic MRI to the knee joint.

REFERENCES

1. Betts AM, Leach JL, Jones BV, Zhang B, Serai S. Brain imaging with synthetic MR in children: clinical quality assessment. *Neuroradiology* 2016; **58**: 1017–26. doi: <https://doi.org/10.1007/s00234-016-1723-9>
2. Granberg T, Uppman M, Hashim F, Cananau C, Nordin LE, Shams S, et al. Clinical feasibility of synthetic MRI in multiple sclerosis: a diagnostic and volumetric validation study. *AJNR Am J Neuroradiol* 2016; **37**:

- 1023–9. doi: <https://doi.org/10.3174/ajnr.A4665>
3. Warntjes JB, Dahlqvist O, Lundberg P. Novel method for rapid, simultaneous T₁, T₂^{*}, and proton density quantification. *Magn Reson Med* 2007; **57**: 528–37. doi: <https://doi.org/10.1002/mrm.21165>
 4. Warntjes JB, Leinhard OD, West J, Lundberg P. Rapid magnetic resonance quantification on the brain: optimization for clinical usage. *Magn Reson Med* 2008; **60**: 320–9. doi: <https://doi.org/10.1002/mrm.21635>
 5. Krauss W, Gunnarsson M, Andersson T, Thunberg P. Accuracy and reproducibility of a quantitative magnetic resonance imaging method for concurrent measurements of tissue relaxation times and proton density. *Magn Reson Imaging* 2015; **33**: 584–91. doi: <https://doi.org/10.1016/j.mri.2015.02.013>
 6. Blystad I, Warntjes JB, Smedby O, Landtblom AM, Lundberg P, Larsson EM. Synthetic MRI of the brain in a clinical setting. *Acta Radiol* 2012; **53**: 1158–63. doi: <https://doi.org/10.1258/ar.2012.120195>
 7. Hagiwara A, Hori M, Suzuki M, Andica C, Nakazawa M, Tsuruta K, et al. Contrast-enhanced synthetic MRI for the detection of brain metastases. *Acta Radiol Open* 2016; **5**: 2058460115626757. doi: <https://doi.org/10.1177/2058460115626757>
 8. Hagiwara A, Hori M, Yokoyama K, Takemura MY, Andica C, Kumamaru KK, et al. Utility of a multiparametric quantitative MRI model that assesses myelin and edema for evaluating plaques, periplaque white matter, and normal-appearing white matter in patients with multiple sclerosis: a feasibility study. *AJNR Am J Neuroradiol* 2017; **38**: 237–42. doi: <https://doi.org/10.3174/ajnr.A4977>
 9. Althawi FF, Blount KJ, Morley NP, Raithe E, Omar IM. Comparing an accelerated 3D fast spin-echo sequence (CS-SPACE) for knee 3-T magnetic resonance imaging with traditional 3D fast spin-echo (SPACE) and routine 2D sequences. *Skeletal Radiol* 2017; **46**: 7–15. doi: <https://doi.org/10.1007/s00256-016-2490-8>
 10. Radlbauer R, Lomoschitz F, Salomonowitz E, Eberhardt KE, Stadlbauer A. MR imaging of the knee: improvement of signal and contrast efficiency of T1-weighted turbo spin echo sequences by applying a driven equilibrium (DRIVE) pulse. *Eur J Radiol* 2010; **75**: e82–e87. doi: <https://doi.org/10.1016/j.ejrad.2009.12.008>
 11. Gold GE, Hargreaves BA, Vasanawala SS, Webb JD, Shimakawa AS, Brittain JH, et al. Articular cartilage of the knee: evaluation with fluctuating equilibrium MR imaging—initial experience in healthy volunteers. *Radiology* 2006; **238**: 712–8. doi: <https://doi.org/10.1148/radiol.2381042183>
 12. Gold GE, Busse RF, Beehler C, Han E, Brau AC, Beatty PJ, et al. Isotropic MRI of the knee with 3D fast spin-echo extended echo-train acquisition (XETA): initial experience. *AJR Am J Roentgenol* 2007; **188**: 1287–93. doi: <https://doi.org/10.2214/AJR.06.1208>
 13. Han CH, Park HJ, Lee SY, Chung EC, Choi SH, Yun JS, et al. IDEAL 3D spoiled gradient echo of the articular cartilage of the knee on 3.0 T MRI: a comparison with conventional 3.0 T fast spin-echo T2 fat saturation image. *Acta Radiol* 2015; **56**: 1479–86. doi: <https://doi.org/10.1177/0284185114556097>
 14. Yamabe E, Anavim A, Sakai T, Miyagi R, Nakamura T, Hitt D, et al. Comparison between high-resolution isotropic three-dimensional and high-resolution conventional two-dimensional FSE MR images of the wrist at 3 tesla: a pilot study. *J Magn Reson Imaging* 2014; **40**: 603–8. doi: <https://doi.org/10.1002/jmri.24428>
 15. Zhang J, Israel GM, Hecht EM, Krinsky GA, Babb JS, Lee VS. Isotropic 3D T2-weighted MR cholangiopancreatography with parallel imaging: feasibility study. *AJR Am J Roentgenol* 2006; **187**: 1564–70. doi: <https://doi.org/10.2214/AJR.05.1032>
 16. Nozaki T, Kaneko Y, Yu HJ, Kaneshiro K, Schwarzkopf R, Yoshioka H. Comparison of T1rho imaging between spoiled gradient echo (SPGR) and balanced steady state free precession (b-FFE) sequence of knee cartilage at 3T MRI. *Eur J Radiol* 2015; **84**: 1299–305. doi: <https://doi.org/10.1016/j.ejrad.2015.03.029>
 17. Landis JR, Koch GG. The measurement of observer agreement for categorical data. *Biometrics* 1977; **33**: 159–74. doi: <https://doi.org/10.2307/2529310>
 18. Jung JY, Yoon YC, Kim HR, Choe BK, Wang JH, Jung JY. Knee derangements: comparison of isotropic 3D fast spin-echo, isotropic 3D balanced fast field-echo, and conventional 2D fast spin-echo MR imaging. *Radiology* 2013; **268**: 802–13. doi: <https://doi.org/10.1148/radiol.13121990>
 19. Jung JY, Yoon YC, Kwon JW, Ahn JH, Choe BK. Diagnosis of internal derangement of the knee at 3.0-T MR imaging: 3D isotropic intermediate-weighted versus 2D sequences. *Radiology* 2009; **253**: 780–7. doi: <https://doi.org/10.1148/radiol.2533090457>
 20. Kijowski R, Davis KW, Woods MA, Lindstrom MJ, De Smet AA, Gold GE, et al. Knee joint: comprehensive assessment with 3D isotropic resolution fast spin-echo MR imaging — diagnostic performance compared with that of conventional MR imaging at 3.0 T. *Radiology* 2009; **252**: 486–95. doi: <https://doi.org/10.1148/radiol.2523090028>
 21. Kijowski R, Davis KW, Blankenbaker DG, Woods MA, Del Rio AM, De Smet AA. Evaluation of the menisci of the knee joint using three-dimensional isotropic resolution fast spin-echo imaging: diagnostic performance in 250 patients with surgical correlation. *Skeletal Radiol* 2012; **41**: 169–78. doi: <https://doi.org/10.1007/s00256-011-1140-4>
 22. Lim D, Han Lee Y, Kim S, Song HT, Suh JS. Clinical value of fat-suppressed 3D volume isotropic spin-echo (VISTA) sequence compared to 2D sequence in evaluating internal structures of the knee. *Acta Radiol* 2016; **57**: 66–73. doi: <https://doi.org/10.1177/0284185114567560>
 23. Park HJ, Lee SY, Rho MH, Chung EC, Ahn JH, Park JH, et al. Usefulness of the fast spin-echo three-point Dixon (mDixon) image of the knee joint on 3.0-T MRI: comparison with conventional fast spin-echo T₂ weighted image. *Br J Radiol* 2016; **89**: 20151074. doi: <https://doi.org/10.1259/bjr.20151074>
 24. Low RN, Austin MJ, Ma J. Fast spin-echo triple echo dixon: Initial clinical experience with a novel pulse sequence for simultaneous fat-suppressed and nonfat-suppressed T2-weighted spine magnetic resonance imaging. *J Magn Reson Imaging* 2011; **33**: 390–400. doi: <https://doi.org/10.1002/jmri.22453>
 25. Andreisek G, White LM, Theodoropoulos JS, Naraghi A, Young N, Zhao CY, et al. Synthetic-echo time postprocessing technique for generating images with variable T2-weighted contrast: diagnosis of meniscal and cartilage abnormalities of the knee. *Radiology* 2010; **254**: 188–99. doi: <https://doi.org/10.1148/radiol.2541090314>
 26. David-Vaudey E, Ghosh S, Ries M, Majumdar S. T₂ relaxation time measurements in osteoarthritis. *Magn Reson Imaging* 2004; **22**: 673–82. doi: <https://doi.org/10.1016/j.mri.2004.01.071>
 27. Dunn TC, Lu Y, Jin H, Ries MD, Majumdar S. T₂ relaxation time of cartilage at MR imaging: comparison with severity of knee osteoarthritis. *Radiology* 2004; **232**: 592–8. doi: <https://doi.org/10.1148/radiol.2322030976>
 28. Kijowski R, Blankenbaker DG, Munoz Del Rio A, Baer GS, Graf BK. Evaluation of the articular cartilage of the knee joint: value of adding a T2 mapping sequence to a routine MR imaging protocol.

- Radiology* 2013; **267**: 503–13. doi: <https://doi.org/10.1148/radiol.12121413>
29. Guermazi A, Alizai H, Crema MD, Trattinig S, Regatte RR, Roemer FW. Compositional MRI techniques for evaluation of cartilage degeneration in osteoarthritis. *Osteoarthritis Cartilage* 2015; **23**: 1639–53. doi: <https://doi.org/10.1016/j.joca.2015.05.026>
30. Nissi MJ, Rieppo J, Töyräs J, Laasanen MS, Kiviranta I, Jurvelin JS, et al. T₂ relaxation time mapping reveals age- and species-related diversity of collagen network architecture in articular cartilage. *Osteoarthritis Cartilage* 2006; **14**: 1265–71. doi: <https://doi.org/10.1016/j.joca.2006.06.002>
31. Joseph GB, Baum T, Alizai H, Carballido-Gamio J, Nardo L, Virayavanich W, et al. Baseline mean and heterogeneity of MR cartilage T₂ are associated with morphologic degeneration of cartilage, meniscus, and bone marrow over 3 years – data from the Osteoarthritis Initiative. *Osteoarthritis Cartilage* 2012; **20**: 727–35. doi: <https://doi.org/10.1016/j.joca.2012.04.003>
32. Mosher TJ, Smith H, Dardzinski BJ, Schmithorst VJ, Smith MB. MR imaging and T2 mapping of femoral cartilage: in vivo determination of the magic angle effect. *AJR Am J Roentgenol* 2001; **177**: 665–9. doi: <https://doi.org/10.2214/ajr.177.3.1770665>